ERODIBILITY EVALUATION OF AN UNLINED ROCK SPILLWAY: COMPARISON BETWEEN THE ERODIBILITY INDEX METHOD AND A NEW METHOD BASED ON BLOCK THEORY

MICHAEL GEORGE[1], COLE CHRISTIANSEN[1], ARIEL RICKEL[1], BENJAMIN ISRAEL[2] AND GEORGE ANNANDALE[3]

[1]BGC Engineering, Inc
701 12th Street, Suite 211, Golden, CO, USA
Contact author e-mail: mgeorge@bgcengineering.com

[2] Gannett Fleming
207 Senate Avenue, Camp Hill, PA, USA
e-mail: bisrael@GFNET.com

[3] George W. Annandale, Inc.
13156 W. Nadine Way, Peoria, AZ, USA
e-mail: george@georgewannandale.com

Key words: unlined spillway, rock scour, Block Theory Rock Erodibility, Erodibility Index Method, CFD, remote sensing.

Summary. Following the 2017 events at the Oroville Dam spillways that prompted evacuation of nearly 200,000 downstream residents and resulted in over $1B USD repair costs, there is highlighted focus on evaluation of spillways (both lined and unlined) at dams across the USA. In the case of unlined channels, flow conditions are often complex which presents several challenges for erodibility evaluation given methods are often based on idealized circumstances. High-resolution data available for the site (both in terms of 3D point cloud geometry data for the rock mass and 3D CFD model simulations of flow conditions) permitted a more detailed analysis of the scouring process, which ultimately provided deeper insight into scour potential. Two methods were used for the analysis; the semi-empirical Erodibility Index Method and a new, physics-based method using Block Theory, and a comparison between the two was made yielding informative results.

1 INTRODUCTION

Spillway erodibility for both lined and unlined channels has received renewed focus following the 2017 events at Oroville Dam in California, USA which resulted in the evacuation of nearly 200,000 downstream residents and over $1B USD in damages and repair costs. Evaluation of unlined spillway channels in rock, in particular, presents several challenges given the wide variations in flow conditions that may exist within the channel at any given time. Existing scour methods have been developed for specific types of flow conditions (plunging jets, plunge pools, channel flow, hydraulic jumps, knickpoints, etc.) which can make direct application of these methodologies to scour assessment of unlined rock spillways difficult as site specific details and conditions can become idealized.

In this paper, we present the use of a computational fluid dynamics (CFD) model along with high-resolution remote sensing data to perform a more detailed, site-specific analysis of the scouring process for an unlined spillway channel in northern California. This analysis made use of the well-known, semi-empirical Erodibility Index Method (Annandale 1995, 2006) as well as a newer physics-based method using Block Theory (George, 2015). The latter examines the removal of discrete rock blocks as defined by the 3D site-specific orientations of discontinuities encountered within the spillway rock mass.

2 SITE OVERVIEW

The spillway site is located in northern California and is founded in hard, moderately jointed, granodioritic rock of the Sierra Nevada Batholith. The spillway was constructed in the 1910's and was situated in a topographic low along the reservoir rim. A defining feature of the unlined spillway is a shear zone within the rock mass running down the center of the channel, parallel to the direction of flow. Over the 100+ year operation of the spillway, had having witnessed discharges up to nearly 950 m^3/s, significant scour has occurred resulting in approximately 510,000 m^3 of material being removed from the channel and the formation of a large slot canyon that has been encroaching on the gated spillway control structure (Figure 1).

Figure 1. Upper reach of eroded slot canyon viewed from middle of spillway (left) and lower reach of slot canyon viewed from below with alluvial fan of scoured material in the foreground (right).

A concrete apron was installed just downstream of the control section in the 1950's to slow the retreat of headward scour toward near the structure. Additional rock bolting and shotcrete was added in the 1990's following the construction of three, lower radial gates on the southern end of the structure. In general, recent scour in the vicinity of the spillway gates has slowed, however, continued deepening of the slot canyon downstream of a large drop in the channel (and much further downstream from the crest) has been visually observed.

3 ROCK ERODIBILITY METHODOLOGY

Two methods were used to assess the scour potential of the unlined spillway: The Erodibility Index Method (EIM) (Annandale 1995, 2006), and the Block Theory Rock Erodibility (BTRE) method (George, 2015). The EIM is a widely accepted semi-empirical method relating material resistance to the erosive capacity of flowing water, while the BTRE approach is a physics-based method to assess stability of a rock mass subject to removal of individual rock blocks under hydraulic loading. For this study, the BTRE method was applied to blocks identifiable at the spillway surface. Both approaches are outlined in the FERC (2018) Engineering Guidelines – Chapter 11 – Arch Dams.

The use of two or more methods is commonly done to provide improved confidence in the estimated scour results. The BTRE approach addresses some shortcomings of the EIM that stem from an empirical representation of the rock mass. Namely, the BTRE methodology incorporates kinematic controls on block stability resulting from the 3D orientations of discontinuities within the rock mass, that are well known to largely influence rock mass behavior (Goodman & Shi 1985).

3.1 Erodibility Index Method

The EIM relates material resistance to the erosive capacity of flow, expressed in unit stream power. When the flow erosive capacity exceeds the material resistance, scour will occur. For rock, the Erodibility Index (K) value representing the material resistance is estimated by Equation 1:

$$K = M_s \cdot K_b \cdot K_d \cdot J_s \tag{1}$$

where M_s = mass strength number (which is function of unconfined compressive strength (UCS) and rock density), K_b = block/particle size number = RQD/J_n where RQD is the rock quality designation and J_n is the joint number, K_d = discontinuity shear strength number = J_r/J_a where J_r is the joint roughness number and J_a is the joint alteration number, and J_s = relative joint structure number (which is a function of joint orientation relative to the flow direction and the shape of rock blocks). Tables for evaluation of each of the above numbers can be found in Annandale (1995, 2006).

Erodibility Index values can be correlated with resisting power (P_r) (kW/m^2) for comparison with the erosive capacity of flow using Equation 2 (Annandale 1995):

$$P_r = K^{0.75} \tag{2}$$

Flow erosive capacity within the spillway is quantified using the unit stream power (SPD) (kW/m^2) which represents the rate of energy dissipation over an area. This is dependent on flow conditions and accordingly, Equation 3 corresponds to jet impingement conditions (either directly on rock or in a plunge pool) and Equation 4 corresponds to channel flow conditions. The unit stream power (SPD) associated with the jet can be expressed as (Annandale 2006).

$$SPD_{jet} = \frac{1}{1000} \cdot \frac{\gamma \cdot q \cdot \Delta E}{d_j} \cdot C_t \tag{3}$$

where γ = unit weight of water (N/m^3), q = unit discharge (m^3/s/m), ΔE = energy head dissipated on the rock mass (m), d_j = jet impact thickness at impact with the rock surface or plunge pool (m), C_t = total dynamic pressure coefficient comprised of C_p (average dynamic pressure coefficient) + C'_p (fluctuating dynamic pressure coefficient) (dimensionless) to account for the degree of break-up as the jet falls through the air as well as the change in erosive capacity of the jet as a function of plunge pool depth (Annandale 2006, Castillo et al. 2015, Castillo & Carillo, 2016).

For energy dissipated under channel flow conditions, the applied unit stream power (kW/m^2) is estimated by Equations 4 and 5. Equation 4 is modified from Annandale's 2006 equation for applied stream power at the channel bed and makes use of the Darcy friction factor:

$$SP_{channel} = \frac{7.853}{1000} \cdot \left(\frac{f}{8}\right)^{\frac{3}{2}} \cdot \rho \cdot u^3 \tag{4}$$

$$f = \left(\frac{1}{2 \cdot \log(12 \cdot R/k)}\right)^2 \tag{5}$$

where u = mean flow velocity (m/s), f = friction factor (dimensionless), ρ = water density (kg/m^3), R = hydraulic radius (assumed ~ flow depth), and k = absolute surface roughness (assumed ~ 1 m) for the conditions analyzed.

Several key locations within the spillway channel were identified for analysis related to the predominant flow conditions (channel flow or jet impingement) anticipated in each region (Figure 2). For channel flow conditions, a 3D CFD model (discussed below) was used directly to estimate flow parameters for estimation of stream power at the location of interest using Equation 4. In other locations where a plunging jet develops, CFD results were only used for the initial jet parameters, with the subsequent erosive capacity estimated analytically using Equation 3 above. Jet locations are located along XS 1a "Lower", XS 2 "Upper", and XS 1b "Slot" (Figure 3). In locations where an impinging jet can form, CFD models typically lack sufficient resolution in modeling air entrainment and jet break-up to provide representative erosive forces, which was judged to be the case here.

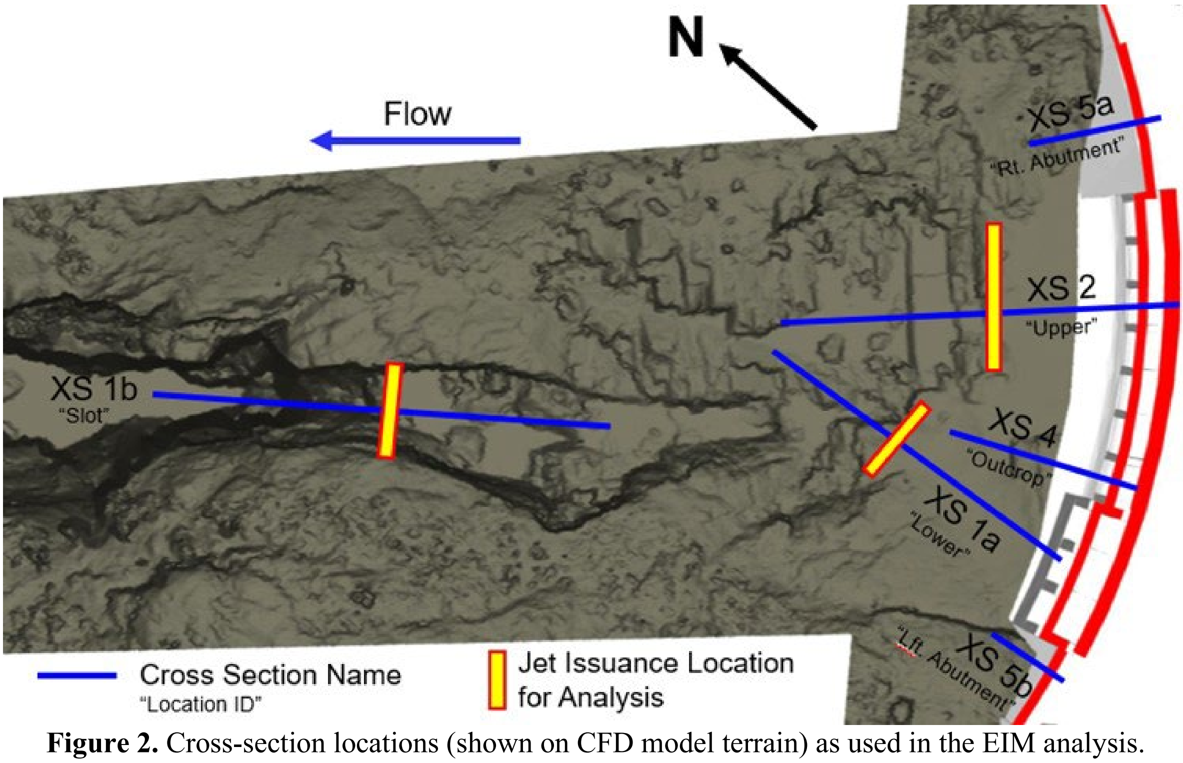

Figure 2. Cross-section locations (shown on CFD model terrain) as used in the EIM analysis.

Figure 3. Cross-sections XS 1a and XS 2 for jets emanating from the concrete apron from the lower and upper spillway gates, respectively (left) and XS 1b for jet emanating from the slot canyon channel.

3.2 Block Theory Rock Erodibility

The BTRE method developed by George (2015) based on Block Theory from Goodman & Shi (1985) was also used to assess spillway erodibility. The Block Theory approach assesses stability of individual blocks pseudo-statically using limit equilibrium. When erosive forces are greater than the rock resisting force, scour will occur.

Hydraulic forces are incorporated into calculation of the active resultant force vector (**R**) which is the vector sum of all active forces applied to the block. For scour analysis, this is namely the hydraulic load and block self-weight. For an 'n-sided' block, this is expressed as:

$$\mathbf{R} = \sum_{i}^{n} P_i \cdot A_i \cdot \mathbf{v}_i + \mathbf{W}_b = \sum_{i}^{n} \frac{1}{2} \cdot \rho \cdot u^2 \cdot C_t \cdot A_i \cdot \mathbf{v}_i + \mathbf{W'}_b \tag{6}$$

where, P_i = hydrodynamic pressure applied to the ith block face (Pa), A_i = area of the ith block face (m^2), $\mathbf{v}_i$ = block side normal unit vector for the ith block face (dimensionless), and $\mathbf{W'}_b$ = vector for the *submerged* block weight (N). Block vector terminology is depicted in Figure 4.

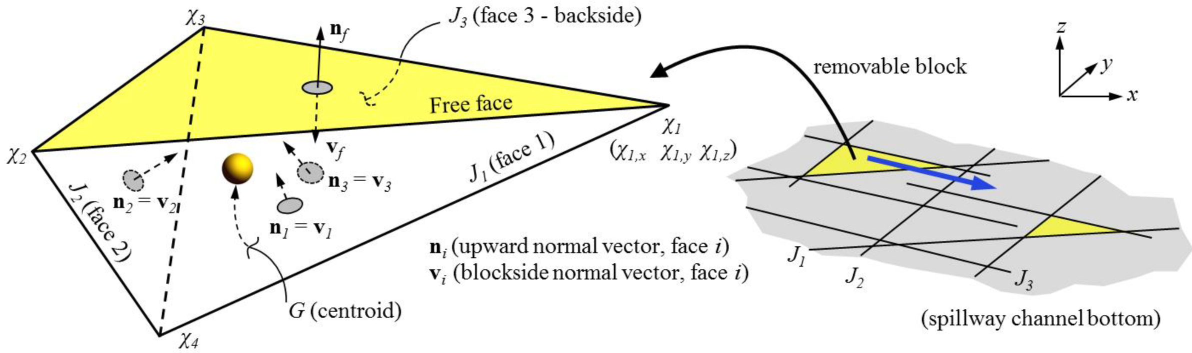

Figure 4. Removable block schematic showing upward block normal vectors (n) and block-side normal unit vectors (v) (George 2015).

Hydrodynamic pressure coefficients (C_p and C'_p) applied to each block face to determine **R** were estimated based on available research for different flow scenarios, which is highlighted in Figure 5. To account for pressure transients that could lead to pressure imbalances around individual rock blocks, C'_p was subtracted from the free block face, while C'_p was simultaneously added to joint faces, which implies a net force associated with pressure fluctuations that is acting to remove the block. Greater transient pressure fluctuations (above the root mean square (RMS), C'_p, values used in the analysis) can exist, however, given the use of a limit equilibrium approach for block stability, it was considered too conservative to use these more extreme pressure fluctuations beyond the RMS values.

For jet impact conditions, either directly onto rock or within a plunge pool, jet theory was used to estimate C_p and C'_p at the top surface of the rock block which corresponds to the rock/air or rock/pool interface. As mentioned above, these values account for the degree of break-up as the jet falls through the air as well as the change in erosive capacity of the jet as a function of plunge pool depth (Annandale 2006, Castillo et al. 2015, Castillo & Carillo, 2016)). Based on research by Federspiel (2011), approximately 35% of C_p and 75% of C'_p at the rock free surface is transmitted to joint faces.

For channel flow conditions with a stepped bed geometry, data from Reinius (1986) was used (as summarized in Bollaert (2012)) to estimate C_p values on block faces. For all blocks within this regime, a downward stepping trend was observed with associated pressure coefficients summarized in Figure 5. To account for turbulence effects, C'_p was estimated based on turbulence intensity (T_u) in the flow field:

$$C'_p=\frac{P'}{P}\sim\frac{1/2\cdot\rho\cdot(u')^2}{1/2\cdot\rho\cdot u^2}=\frac{(u')^2}{u^2}=T_u^2 \tag{7}$$

where u′ = the fluctuating flow velocity (m/s).

For channel flow on a planar surface, research by George (2015) was used to relate the flow velocity vector (**u**) to the orientation of the upstream block faces and the protrusion of the block (h) above the channel bed. Empirical relationships for C_p were applied based on laboratory testing under ‘high’ turbulence conditions. Accordingly, application of C'_p was not required for these conditions.

Block stability under hydraulic loading is assessed in a pseudo-static manner using the standard Block Theory limit equilibrium vector equations outlined by Goodman & Shi (1985). These equations relate to the different kinematic failure modes (e.g., lifting, 1-plane sliding, 2-plane sliding) for a given block geometry. The kinematic modes are highly dependent on the 3D orientations of the discontinuities planes bounding the block as well as the orientation(s) of the free surface(s) defining the block. Accordingly, block kinematics result in a three-dimensional block resistance to scour which is important to account for when assessing erodibility potential. From Block Theory, stability is evaluated by determining the scalar value of the required stabilizing force (F) that is applied in the direction of block movement to maintain limit equilibrium. For a block lifting from all joint planes,

$$F=|\mathbf{R}|, \tag{8}$$

for block sliding on 1 joint plane (i),

$$F_i=|\mathbf{n}_i\times\mathbf{R}|-|\mathbf{n}_i\cdot\mathbf{R}|\cdot\tan(\phi_i),\text{ and} \tag{9}$$

Jet Impact (Direct/Plunge Pool)

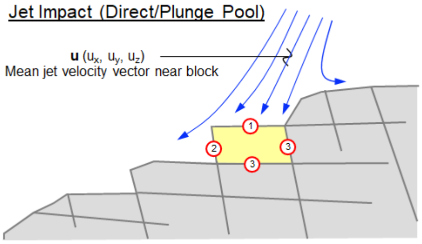

Face Location	Avg. & Fluc. Dynamic Pressure Coef.	Total Pressure Coef.	Notes
① Free Face (impact):	$C_p = C_{p\_surf/pool}$ $C'_p = C'_{p\_surf/pool}$	$C_t = C_p - C'_p$	$C_{p\_surf/pool}$ & $C'_{p\_surf/pool}$ estimated at rock air/pool surface interface based jet break-up and plunge pool jet theory.
② Free Face (no impact):	$C_p = 0$ $C'_p = 0$	$C_t = 0$	
③ Joint Face:	$C_p = 0.35 \cdot C_{p\_surf/pool}$ $C'_p = 0.75 \cdot C'_{p\_surf/pool}$	$C_t = C_p + C'_p$	0.35 & 0.75 reduction factors for joint pressures based on testing from Federspeil (2011) for jet impact on a rock block

Bed Parallel Flow (Downward Step)

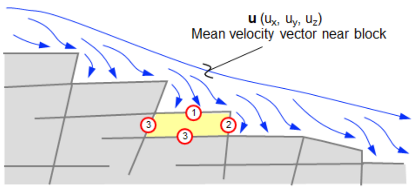

Face Location	Avg. & Fluc. Dynamic Pressure Coef.	Total Pressure Coef.	Notes
① Free Face (top):	$C_p = 0.08$ $C'_p = T_u^2$	$C_t = C_p - C'_p$	C_p on top free face and joint face estimated based on research by Reinius (1986) as summarized by Bollaret (2012)
② Free Face (side):	$C_p = 0$ $C'_p = 0$	$C_t = 0$	C'_p estimated based on flow turbulence intensity (T_u). Reinius (1986) provides average uplift pressures.
③ Joint Face:	$C_p = -0.11$ $C'_p = T_u^2$	$C_t = C_p + C'_p$	Additional geometries summarized in Reinius (1986) and Bollaert (2012).

Bed Parallel Flow (Planar)

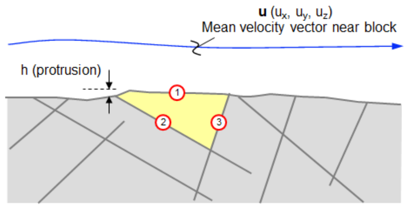

Face Location	Avg. & Fluc. Dynamic Pressure Coef.	Total Pressure Coef.	Notes
① Free Face (top):	$C_p = 0.005$ $C'_p = NA$	$C_t = C_p$	C_p estimated based on emperical relationships developed by George (2015) as a function of block orieintation (Ψ) with respect to flow direction (**u**) and block protrusion height (h).
② Joint Face (u/s):	$C_p = f(\Psi, \mathbf{u}, h)$ $C'_p = NA$	$C_t = C_p$	C'_p not estimated as C_p values based on 'High' turbulence condition from George (2015).
③ Joint Face (d/s):	$C_p = f(\Psi, \mathbf{u}, h)$ $C'_p = NA$	$C_t = C_p$	Protrusion (h) based on bed roughness in block vicinity if could not be measured directly.

Figure 5. Hydrodynamic pressures coefficients for estimation of hydraulic forces applied to removable rock blocks based on dominant flow condition.

for block sliding on 2 joint planes (i and j),

$$F_{ij} = \frac{1}{\left|\mathbf{n}_i \times \mathbf{n}_j\right|^2} \cdot \left[\begin{array}{c} \left|\mathbf{R}\cdot(\mathbf{n}_i \times \mathbf{n}_j)\right| \cdot \left|\mathbf{n}_i \times \mathbf{n}_j\right| - \\ \left|(\mathbf{R}\times\mathbf{n}_j)\cdot(\mathbf{n}_i \times \mathbf{n}_j)\right| \cdot \tan(\phi_i) - \\ \left|(\mathbf{R}\times\mathbf{n}_i)\cdot(\mathbf{n}_i \times \mathbf{n}_j)\right| \cdot \tan(\phi_j) \end{array} \right] \quad (10)$$

where ϕ_i, ϕ_j = friction angle (deg.) on joints (block faces) i and j, respectively, and **n** is upward normal unit vector on joint plane (block face) i (Figure 4).

When F is negative the block is considered stable, and when F is positive the block is unstable. When F is zero, the block is in equilibrium such that any further increase in load will result in removal of the block. Additional information on Block Theory analysis can be found in Goodman & Shi (1985) and George (2015).

For the unlined spillway channel at the project site, high-resolution remote sensing data collected from both ground-based LiDAR as well as UAV photogrammetry were used to facilitate analysis of specific rock blocks identifiable in the surface of the spillway channel using the BTRE method.

The spillway point cloud was viewed using the open-source software CloudCompare. Removeable blocks (i.e., blocks in the rock mass which are kinematically capable to be eroded from the rock mass) were visually identified in the point cloud. CloudCompare's built-in tools were used to extract the orientations and locations of each face defining the block of interest. Block faces within the rock mass that were not visible were delineated using 1) expressions of the same joint plane at a nearby location to the block or 2) the expression of the linear trace of the block face at the surface. A Matlab script was developed to generate a 3D digitized block based on the measurements made in CloudCompare that would output the required block data for BTRE analysis, which included: block-side normal vector (**v**) for each block face, block face area (A) and block volume (V_b).

All removeable, digitized rock blocks from the spillway channel that were analyzed for the scour assessment are shown in Figure 6 and Figure 7. Note that not every single removeable block from the spillway was digitized. The goal was rather to analyze only a select number of representative blocks in key locations throughout the spillway to inform if scour was likely or not. In all, 24 blocks were digitized. Blocks were predominantly located in the upstream portion of the spillway channel were the point cloud density and resolution were highest.

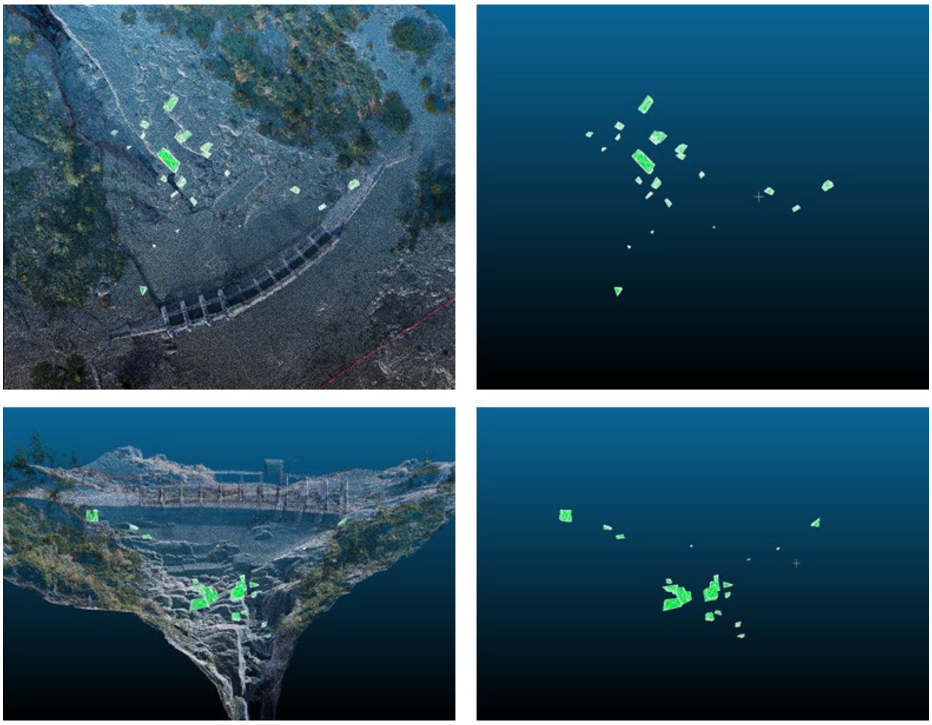

Figure 6. Digitized 3D rock blocks in spillway channel from point cloud data for use in erodibility analysis with the BTRE methodology.

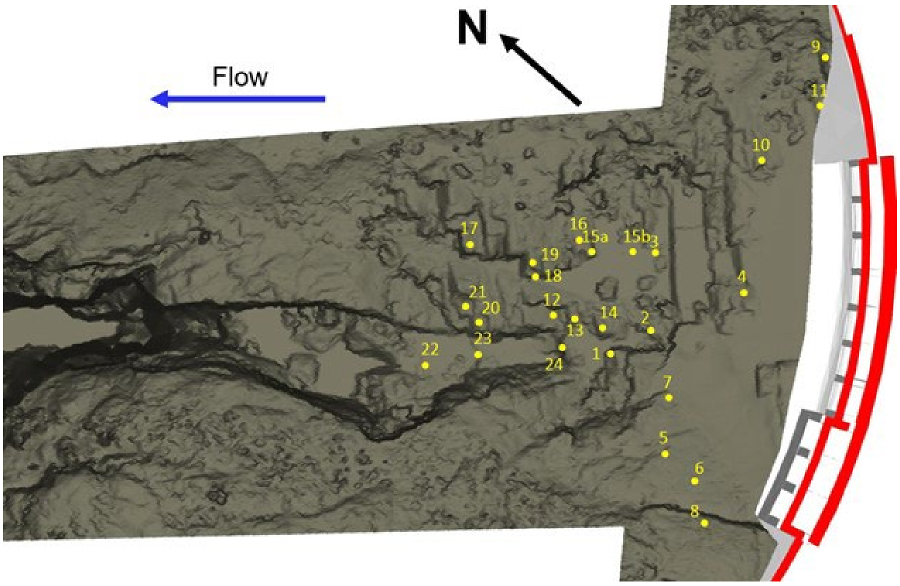

Figure 7. Digitized 3D rock blocks locations on top of CFD model terrain.

3.3 3D Computational Fluid Dynamics Model

A 3D CFD model was developed for the spillway site to assist in the evaluation of flow erosive capacities using the commercial Flow3D software by FlowScience. This was a necessity given limitations of other analytical and numerical tools (i.e., 1D and 2D hydraulic models) to adequately capture the complex nature of the flow conditions in the channel.

The LiDAR point cloud data used for block digitization was also used to generate the CFD model terrain. A 0.3 m grid spacing was used to define the domain of the rock mass downstream of the spillway gates in the model. Steady state models were developed for several spillway discharge conditions corresponding to historic flows for model validation as well as design flow conditions. Models used a Reynolds Averaged Navier Stokes (RANS) turbulence model which considers both mean and fluctuating fluid motions.

Data from the model (velocity magnitude and vector, flow depth, and turbulence intensity) were extracted at several locations relevant to the scour analysis. Figure 8 shows CFD model output at the jet issuance location along XS 2 (Figure 2) that was used as input into the analytical jet scour model for use with the EIM (a schematic of which is also shown in Figure 8).

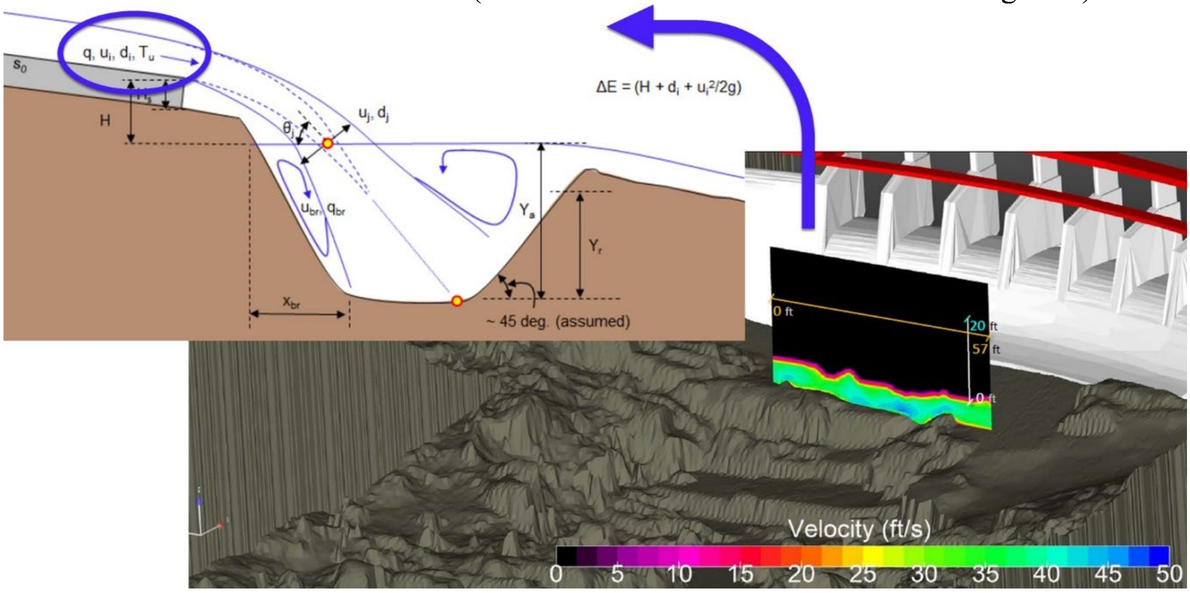

Figure 8. CFD model output at jet issuance location along XS 2 (right) for a spillway discharge of 850 m3/s used as input into the analytical jet scour model.

Figure 9 shows digitized rock blocks in the spillway channel along with flow streamlines and velocity data output from the CFD model. With the CFD model, it was possible to extract site-specific flow conditions at each digitized block location in order to determine the hydraulic load applied to each block and analyze block stability using the BTRE method.

4 ANALYSIS OF THE RESULTS

4.1 Erodibility Index Method

A plot comparing the estimated rock Erodibility Index (K) values to the estimated stream power of the flowing water is shown in Figure 10 where data is superimposed on Annandale's original Erodibility Index graph. This was done for four separate spillway discharges: 425 m^3/s (15,000 ft^3/s), 850 m^3/s (30,000 ft^3/s), 1,415 m^3/s (50,000 ft^3/s), and 1,980 m^3/s (70,000 ft^3/s) at each location shown in Figure 2. The plot shows the threshold scour line and when data plot above the threshold, scour is considered to occur.

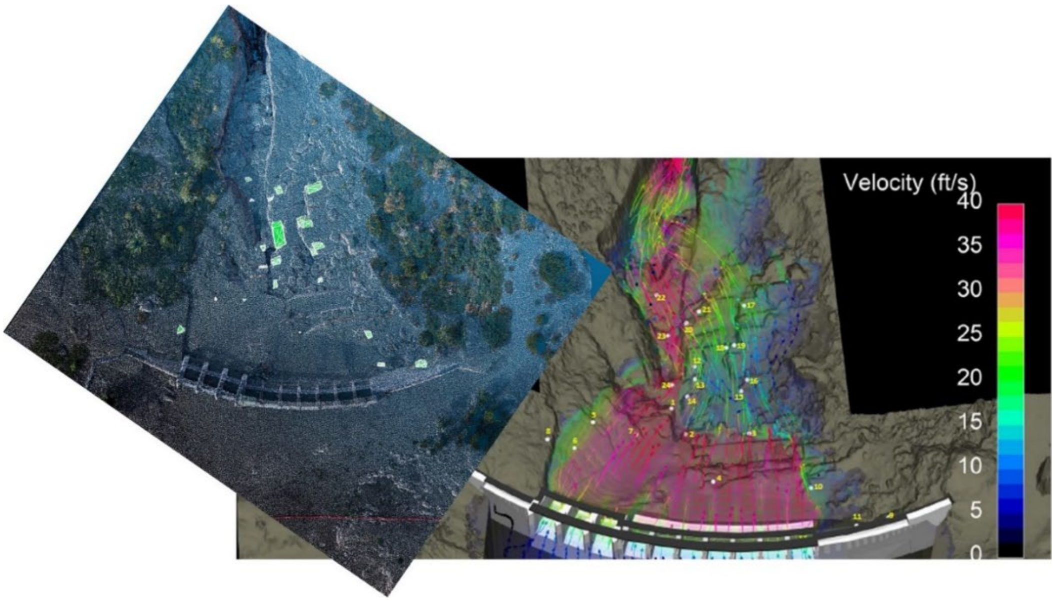

Figure 9. Digitized 3D rock blocks in spillway channel (left) and flow velocity output from CFD model showing block locations (right) for 565 m^3/s discharge.

Erodibility Index (K) value were estimated to be K = 4,766 (P_r =574 kW/m^2) for intact granodiorite bedrock and K = 34 (P_r = 14 kW/m^2) for fractured material in the shear zone region forming the slot canyon. The intact bedrock has considerable scour resistance and is only shown to be erodible in the slot canyon downstream of a large drop in the channel (green markers) which is consistent with visual observations from the site. Two-dimensional scour hole profiles were also developed for this location but are not presented here. No other locations of intact bedrock were estimated to be erodible with the EIM analysis.

Rock in the shear zone is more susceptible to scour occurring where jet conditions develop from flow existing the lower spillway gates (navy blue markers) and where channel flow exists in the slot canyon (red markers). This also agrees with site observations as the majority of material eroded from the spillway has come from the shear zone region.

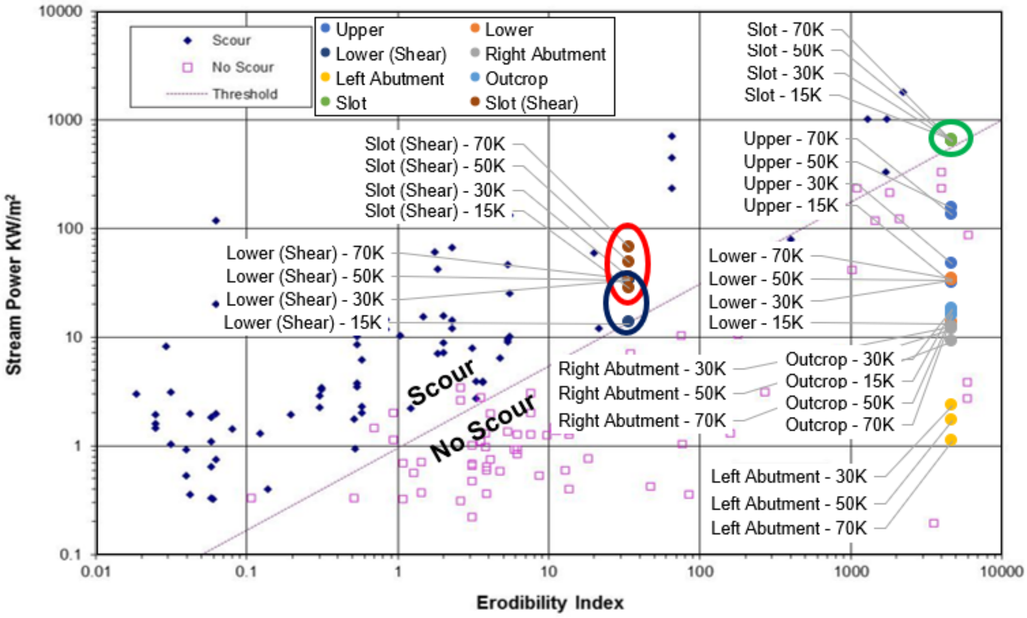

Figure 10. EIM results for the unlined spillway channel superimposed on Annandale's Erodibility Index graph. Conditions where scour is anticipated to occur are circled.

4.2 Block Theory Rock Erodibility

Predictive BTRE stability results for each of the digitized rock blocks in the spillway channel under discharge conditions of 425 m^3/s (15,000 ft^3/s), 850 m^3/s (30,000 ft^3/s), 1,415 m^3/s (50,000 ft^3/s), and 1,980 m^3/s (70,000 ft^3/s) are shown in Table 1. A number of blocks were excluded from the table. Blocks 4, 7, 12 were used in back-analysis / validation of the BTRE method for historic spillway discharges, while Block 6 could not be digitized from the point cloud due to low point density in the block region.

Table 1. Predictive results for BTRE analysis of spillway rock blocks.

<table>
<tr><th rowspan="2">Block</th><th rowspan="2">Location ID</th><th rowspan="2">Flow Condition</th><th colspan="4">Spillway Discharge</th></tr>
<tr><th>425 m³/s</th><th>850 m³/s</th><th>1415 m³/s</th><th>1980 m³/s</th></tr>
<tr><td>1</td><td>Lower/Slot</td><td>Channel (step)</td><td style="background:green"></td><td style="background:green"></td><td style="background:green"></td><td style="background:green"></td></tr>
<tr><td>2</td><td>Lower/Slot</td><td>Jet</td><td style="background:green"></td><td style="background:green"></td><td style="background:green"></td><td style="background:green"></td></tr>
<tr><td>3</td><td>Upper</td><td>Jet</td><td style="background:green"></td><td style="background:green"></td><td style="background:green"></td><td style="background:green"></td></tr>
<tr><td>5</td><td>Lower</td><td>Channel (planar)</td><td style="background:red"></td><td style="background:red"></td><td style="background:red"></td><td style="background:red"></td></tr>
<tr><td>8</td><td>Left Abutment</td><td>Channel (planar)</td><td style="background:green"></td><td style="background:green"></td><td style="background:green"></td><td style="background:green"></td></tr>
<tr><td>9</td><td>Right Abutment</td><td>Jet</td><td style="background:green"></td><td style="background:green"></td><td style="background:green"></td><td style="background:green"></td></tr>
<tr><td>10</td><td>Upper</td><td>Channel (planar)</td><td style="background:green"></td><td style="background:green"></td><td style="background:green"></td><td style="background:green"></td></tr>
<tr><td>11</td><td>Right Abutment</td><td>Jet</td><td style="background:green"></td><td style="background:green"></td><td style="background:green"></td><td style="background:green"></td></tr>
<tr><td>13</td><td>Lower/Slot</td><td>Jet</td><td style="background:red"></td><td style="background:red"></td><td style="background:green"></td><td style="background:green"></td></tr>
<tr><td>14</td><td>Lower/Slot</td><td>Jet</td><td style="background:red"></td><td style="background:red"></td><td style="background:green"></td><td style="background:green"></td></tr>
<tr><td>15a</td><td>Upper</td><td>Channel (planar)</td><td style="background:green"></td><td style="background:green"></td><td style="background:green"></td><td style="background:green"></td></tr>
<tr><td>15b</td><td>Upper</td><td>Jet</td><td style="background:red"></td><td style="background:red"></td><td style="background:red"></td><td style="background:green"></td></tr>
<tr><td>16</td><td>Upper</td><td>Channel (planar)</td><td style="background:green"></td><td style="background:green"></td><td style="background:green"></td><td style="background:green"></td></tr>
<tr><td>17</td><td>Upper</td><td>Channel (step)</td><td style="background:green"></td><td style="background:green"></td><td style="background:green"></td><td style="background:green"></td></tr>
<tr><td>18</td><td>Upper/Lower</td><td>Channel (step) / Jet (30K cfs)</td><td style="background:green"></td><td style="background:green"></td><td style="background:green"></td><td style="background:green"></td></tr>
<tr><td>19</td><td>Upper</td><td>Channel (step)</td><td style="background:green"></td><td style="background:green"></td><td style="background:green"></td><td style="background:green"></td></tr>
<tr><td>20</td><td>Slot (Edge)</td><td>Channel (step)</td><td style="background:green"></td><td style="background:green"></td><td style="background:green"></td><td style="background:green"></td></tr>
<tr><td>21</td><td>Slot (Edge)</td><td>Channel (step)</td><td style="background:green"></td><td style="background:green"></td><td style="background:green"></td><td style="background:green"></td></tr>
<tr><td>22</td><td>Slot</td><td>Channel (step)</td><td style="background:green"></td><td style="background:green"></td><td style="background:green"></td><td style="background:green"></td></tr>
<tr><td>23</td><td>Slot</td><td>Channel (step)</td><td style="background:green"></td><td style="background:green"></td><td style="background:green"></td><td style="background:green"></td></tr>
<tr><td>24</td><td>Lower/Slot</td><td>Jet</td><td style="background:green"></td><td style="background:green"></td><td style="background:green"></td><td style="background:green"></td></tr>
</table>

<table>
<tr><td style="background:green"></td><td>Block is Stable</td></tr>
<tr><td style="background:red"></td><td>Block is Unstable</td></tr>
</table>

For Block 15, stability assessment was made for two flow conditions assuming 1) channel flow on a planar surface, and 2) jet impingement. For the latter, the block was assumed to reside further upstream and would be subject to jet impact from flow emanating from the concrete apron below the upper spillway gates. For Block 20, stability assessment was made for 1-plane sliding only as the block only has one face in contact with rock mass.

A discontinuity friction angle of ϕ = 66 degrees was used to represent discontinuity shear strengths for the rock blocks, which was determined from testing of rock samples from site.

Results indicate the majority of blocks analyzed are stable under the full range of flow conditions considered, which shows good agreement with the EIM. Scour of intact rock adjacent to the shear zone in the upper portion of the slot canyon, however, was assessed to be unlikely using the EIM (Figure 10, "Lower"), while the BTRE approach indicates that rock at this location is susceptible to plucking of individual blocks. Block scour appears to be most dominant at lower discharges ($\leq$ 850 m^3/s) which was hypothesized to be attributed to the jet emanating from the apron at higher flows with less turbulence, which reduces the potential for large pressure fluctuations and imbalances on the block. However, because large flow events also must pass through lower flow regimes during ramp up and down of the event hydrograph, blocks could still be at risk for scour during higher spillway discharge events.

BTRE results are supported by observations using repeated monitoring with high-resolution LiDAR scans of the spillway. Change detection analysis between datasets show that some individual blocks have been removed in this region over a period of approximately 7 years leading up to the scour analysis.

The difference in results at the slot canyon margin between the EIM and BTRE methods is of interest and is attributed to rock block kinematics. Block kinematic conditions are accounted for in BTRE, but not the EIM. Scour of the weaker shear zone material in the slot canyon creates void space adjacent to the intact bedrock forming the slot canyon wall. This space allows rock blocks in the wall more kinematic freedom to move which can result in a lower erodibility threshold of the blocks. This is shown in Figure 11.

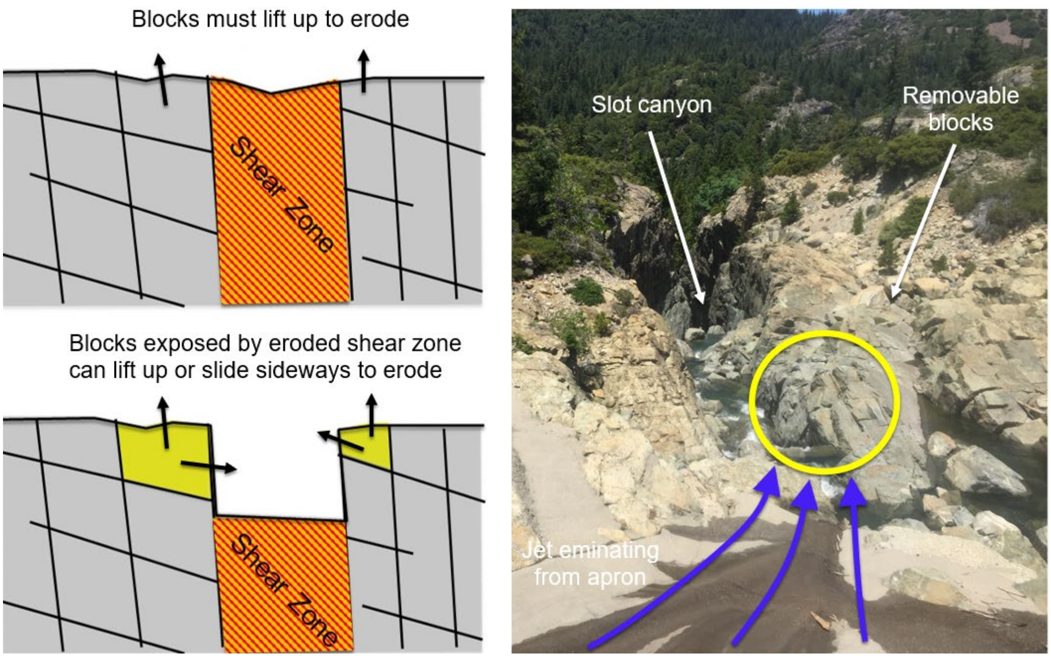

Figure 11. Schematic showing influence of eroded shear zone on block kinematic failure modes (left) and view of the slot canyon and location of interest in the canyon wall subject jet impingement flows from the lower spillway gates.

This result is particularly insightful as continued scour of the shear zone allows exposure of additional ‘removeable’ rock blocks (i.e., blocks that can physically move into a void space), which is required for scour progression in the intact rock mass to occur. As long as the shear zone continues to erode, the surrounding intact rock mass will be susceptible to scour at this location. The limited number of blocks observed to be eroded using LiDAR change detection suggests that the rate of future scour progression in the intact material would be sufficiently slow to allow time for intervention and mitigation.

5 CONCLUSIONS

Erodibility analysis of unlined rock spillways can be challenging given 1) the complex geometries in the rock mass that exist (or can develop) as influenced by the 3D rock discontinuity orientations and 2) the variety of flow conditions that can be encountered at any given time in the channel. Given these complexities, site-specific details can get lost or generalized when using existing scour methodologies that are often developed under idealized conditions.

This paper presents a new physics-based approach based on Block Theory to analyze scour of individual rock blocks in the spillway. The BTRE method incorporates the site-specific, 3D orientations of rock mass discontinuities that define block geometries in order to assess erodibility potential. Block geometries can be generated more generally based on known joint orientations in the rock mass or more specifically using block specific measures derived from remote sensing data of the rock mass surface. For this study, actual 3D rock blocks in the surface of the spillway channel were digitized using high-resolution remote sensing point cloud data obtained from ground-based LiDAR and UAV photogrammetry. A 3D CFD model was also used to determine specific flow conditions at each block location in order to assess hydraulic loading on the block and ultimately block stability for several different spillway discharges.

The use of the remote sensing data and the CFD model with the BTRE methodology allowed a more detailed, site-specific assessment of scour than has been previously attenable. The BTRE analysis results were compared with those obtained from the EIM and were generally agreeable. One notable exception were blocks located at the margins of the slot canyon which were predicted to be erodible using the BTRE method but not with the EIM.

At that location, blocks have more kinematic liberty to be removed from the rock mass given weaker material in the shear zone had been previously eroded creating additional space into which the blocks can move. Previous scour of similar block types in the same location was confirmed through change detection analysis of a series of LiDAR scans taken of the spillway channel over a period of approximately 7 years. This highlights the importance of considering block kinematics on erodibility potential.

The approach incorporating high-resolution remote sensing data and 3D CFD used with the BTRE method can be readily transferable to other spillway locations to provide improved resolution for scour estimates of individual rock blocks as well as additional insight into the scouring process. The use of both methods (BTRE and EIM) together is suggested to provide improved confidence in the scour results.

REFERENCES

Annandale, G.W. (1995). ‘Erodibility’. J. Hyd. Research, 33(4): 471-494.

Annandale, G.W. (2006). Scour technology: mechanics and engineering practice, New York, McGraw-Hill.

Bollaert, E.F.R. (2012). 'Wall jet rock scour in plunge pools: a quasi-3D prediction model'. Hydropower & Dams, Issue XX.

Castillo, L.G. and Carrillo, J.M. (2016). 'Pressure and velocity distributions in plunge pools', 2nd International Seminar on Dam Protection Against Overtopping, Fort Collins, Colorado, USA.

Castillo, L.G., Carrillo, J.M. and Blazquez, A. (2015). 'Plunge pool mean dynamic pressures: A temporal analysis in nappe flow case', J. Hyd. Research, 53(1): 101-118.

Federspiel, M. (2011). 'Response of an embedded block impacted by high-velocity jets, Communication No. 47'. Ph.D. Dissertation. Laboratory of Hydraulic Constructions. Ecole Polytechnique Federale de Lausanne, Switzerland.

FERC (2018). 'Engineering guidelines for the evaluation of hydropower projects - Chapter 11: Arch dams'. Washington, DC: Federal Energy Regulatory Commission.

George, M.F. (2015). '3D block erodibility: Dynamics of rock-water interaction in rock scour'. Ph.D. Dissertation. UC-Berkeley.

Goodman, R.E. and Shi, G. (1985). Block theory and its application to rock engineering, Englewood Cliffs, NJ, Prentice Hall.

Reinius, E. (1986). 'Rock erosion'. Water Power and Dam Construction, (June): 43-48.